Tellus (2007), 59B, 66–76

TELLUS

Factors influencing the mesoscale variations in marine stratocumulus albedo

By D. A. HEGG[1]*, K. NIELSEN[2], D. S. COVERT[1], H. H. JONSSON[2,3] and P. A. DURKEE[2],
[1]*Department of Atmospheric Sciences, MS 351640 University of Washington, Seattle, WA USA;* [2]*Department of Meteorology, Naval Postgraduate School, Monterey, CA, USA;* [3]*Center for Interdisciplinary Remotely Piloted Aircraft Studies, Naval Postgraduate School, Monterey, CA, USA*

(Manuscript received 1 February 2006; in final form 28 September 2006)

ABSTRACT

Measurements of both horizontal gradients and vertical profiles of aerosols, cloud droplets and thermodynamic parameters in the cloud topped marine boundary layer off of central California are presented. They suggest that, while aerosols can indeed modulate cloud albedo, other parameters such as sea surface temperature may similarly affect cloud albedo. Additionally, the impact of aerosols, through sedimentation and precipitation, on cloud optical depths and thus albedo is not always in accord with conventional expectations and can either enhance or decrease the albedo, depending on ambient conditions. Taken together, these results suggest that current estimates of indirect forcing by aerosols could be significantly in error.

1. Introduction

Numerous studies have proposed indirect aerosol forcing (i.e., aerosol forcing through modulation of cloud albedo) as an important factor in the energy balance of the earth-atmosphere system (e.g., Twomey, 1974, 1991; Charlson et al., 1987; Albrecht, 1989). Measurements on the global scale do in fact suggest that aerosols impact cloud albedo (Han et al., 1994) and very local measurements (on the order of a few km) have demonstrated the reality of the aerosol-cloud droplet size – albedo effect first postulated by Twomey and now referred to as the Twomey effect (cf. Brenguier et al., 2000). Similarly, there is some evidence on local scales that the cloud drop number – precipitation – albedo relationship proposed by Albrecht (1989) – Albrecht effect – does occur (Ferek et al., 2000). However, it is the mesoscale variability in cloud albedo that contributes most to the overall albedo variance of cloud systems (Rossow et al., 2002), and on this scale a number of factors other than aerosols (e.g., sea surface temperature, SST as per Wyant et al., 1997; dry continental air advection as per Brenguier et al., 2003) can influence the cloud thermodynamics, possibly sufficiently to result in a net impact on cloud albedo substantially less than expected if only aerosols were exerting influence. Observations yield a less than clear-cut picture. For example, Sekiguichi et al. (2003), using mesoscale satellite retrievals, found highly variable (including both positive and negative) correlations between aerosol number concentration and retrieved cloud drop effective radius rather than the expected strong negative correlation of the Twomey effect. Shao and Liu (2005) have interpreted this in terms of unexpected correlations between cloud geometric thickness and aerosol number concentration. Similarly, Brenguier et al. (2003) report negative correlations between cloud geometric thickness and aerosol number concentration for the ACE-2 campaign, which they attribute primarily to mixing of relatively fresh continental air and marine air rather than a purely aerosol relationship. Recently, aerosol indirect forcings (e.g., Ackerman et al., 2004) have also been suggested that have quite different impacts from conventional mechanisms. The rationalization of Brenguier et al. could have strong implications for the magnitude of aerosol forcing. And, of course, it should not be forgotten that not only can aerosols impact clouds but the converse is also true, specifically for marine stratocumulus (cf. Hudson and Frisbie, 1991). This reciprocity should always be considered when interpreting observations.

Marine stratocumulus decks play a major role in determining planetary albedo and tend to be located along the eastern peripheries of the major oceans (Warren et al., 1988). They will all experience a mixture of continental and marine air. Along these lines, Shao and Liu (2005) found different relationships between the aerosol (non-cloud) optical depth – a surrogate for aerosol number concentration – and cloud geometric thickness as a function of distance from the coastline, with the near-shore data in agreement with the findings of Brenguier et al. (2003).

*Corresponding author.
e-mail: deanhegg@atmos.washington.edu
DOI: 10.1111/j.1600-0889.2006.00231.x

These analyses therefore suggest an interesting compensating influence to aerosol impact on cloud albedo, namely, that the offshore flow necessary to bring polluted air with higher aerosol concentrations into the marine environment, and implement the Twomey or Albrecht effects, will simultaneously advect drier air leading to smaller geometric cloud thickness.

Finally, there are mechanisms that modulate cloud albedo independently of aerosol concentration. Indeed, for the marine stratocumulus decks so important to large-scale radiative forcing (and from which much of the data discussed above is derived), it has long been understood that it is SST more than perhaps any other variable that modulates overall cloud optical depth and albedo (cf. Klein et al., 1995; Bretherton and Wyant, 1997; Pincus et al., 1997), certainly for the synoptic scale. (It is noteworthy that up until the point where SST's are sufficiently high to lead to the Sc to Cu transition, the correlation between SST and albedo is generally positive.) Furthermore, Hegg et al. (2004) have shown that stratocumulus albedo variations on the mesoscale can also be attributed to SST gradients. It is entirely conceivable that aerosol gradients induced by pollution but in contrary senses to SST gradients might have little impact on cloud albedo.

In light of these issues, we have gathered and analyzed both in situ data on aerosols and cloud microphysics, and remotely retrieved cloud albedo's and SST's from the region of extensive marine stratocumulus cloud off of the central California coast. The measurements were made during July and August of 2004 and 2005 as part of the Cloud Aerosol Research in the Marine Atmosphere (CARMA-II and CARMA-III) campaigns, respectively. Our goal is to clarify which factors have a significant impact on the mesoscale variability in marine stratocumulus albedo, and, if possible, to quantify the relative importance of these factors.

2. Observational plan

2.1. Experimental venue

The geographic location of the measurements reported here is shown in Fig. 1a. They were thus centred in one of the handful of persistent (and uniform) marine stratocumulus decks found globally. Furthermore, numerous studies of this venue have demonstrated, primarily in ship tracks, that indirect aerosol forcing can and does occur (e.g., Platnick and Twomey, 1994; Durkee et al., 2000). The location features both mesoscale gradients in aerosol concentration and in SST, gradients that are sometimes orthogonal (cf. Hegg et al., 2004).

2.2. The aircraft platform

All of the in situ data described here were obtained with the CIRPAS Twin Otter aircraft instrumentation package. Most components of this package have been described in a number of previous publications (cf. Hegg et al., 2002; Wang et al., 2002) but, perhaps with most relevance to this study, Hegg et al. (2004). Recapitulating the portions of these discussions relevant to the current analysis, the PMS/DMT PCASP-100 (size range: $0.12 < d < 3.2\ \mu$m) was the primary tool employed for aerosol measurement, the PMS/DMT FSSP-100 and the DMT CAPS probe were used for cloud drop and drizzle drop concentration, respectively, and SST was measured by means of a Heitonics IR thermometer (model KT 19-85). Additionally, for CARMA-III (2005), a Gerber PVM-100 was available for measurement of the liquid water mixing ratio, a more reliable technique than integration of the FSSP-100 size distribution (employed in CARMA-II). While the PVM-100 also provides a measure of the integral cloud drop scattering crossection, and thus of the effective radius, this output proved much less reliable, yielding values incompatible with various other measurements. Hence, for effective radius determination, we use the PVM-100 liquid water data coupled with the FSSP cloud drop number concentration (CDNC) to derive the volume mean radius and then use a scaling factor of 0.95 to relate the effective radius to the volume mean radius (cf. Martin et al., 1994; Brenguier et al., 2003).

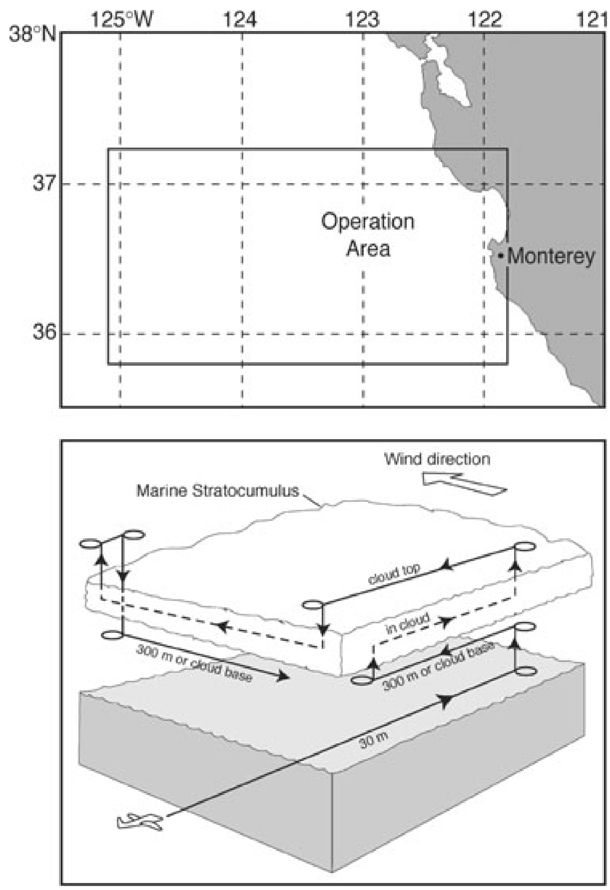

Fig. 1. (a) Geographic location for the CARMA studies and (b) sampling flight plan for the study.

Table 1. Summary of the horizontal traverses obtained during the CARMA-II and CARMA-III campaigns

Flight number	Date	Traverse length (km)	Number of vertical profiles	Time of day (UTC)	Aerosol–r_{tot} correlation	Aerosol–MSE correlation
708	July 8, 2004	38	2	1716	–0.10	–0.02
709	July 9, 2004	58	2	1910	0.09	0.2
710	July 10, 2004	40	2	1718	–0.06	–0.05
712	July 12, 2004	86	2	1728	0.07	–0.17
713	July 13, 2004	95	2	1811	–0.13	0.0
721	July 21, 2004	110	2	1813	–0.24	–0.19
810	August 10, 2005	91	1	1810	0.19	0.18
816	August 16, 2005	48	2	2019	–0.68	–0.77
818	August 18, 2005	121	1	1702	–0.10	–0.13
819	August 19, 2005	121	0	1728	–0.04	0.08
824	August 24, 2005	101	1	1848	0.02	0.14
826	August 26, 2005	121	2	1958	0.41	0.84

2.3. *Satellite retrievals*

Satellite remote sensors were used to retrieve the cloud albedo along the flight tracks where the Twin Otter sampled in or near cloud. The sensors used were the AVHRR radiometer in the NOAA 15, 16 and 17 satellites and the standard spectral radiometer employed on the GOES-10 (West) satellite (channel 1, 0.63 μm). Both radiometers have been described in previous studies (e.g., Rao et al., 1999). The absolute accuracy of the albedo's retrieved by these radiometers, particularly that on GOES-10, is uncertain but we utilize them here primarily to establish spatial trends and for this only relative accuracy is essential.

2.4. *Sampling plan*

The two prospective forcing factors for cloud albedo that might reasonably be considered external, and thus susceptible to determination independently of the stratiform cloud deck itself, are aerosol concentration and SST. Mesoscale gradients in these variables are indeed present in the operational area and have previously been associated with albedo gradients (Hegg et al., 2004). Hence, flight legs were conducted below cloud along paths where either SST or aerosol gradients might be expected. When gradients were in fact found, the flight legs were extended for about 20 min duration (spatial scale of ~60 km) directly along the gradient, if possible, but always more or less perpendicular to the mean wind – even at the cost of some attenuation in the gradient. This was done so that the local properties along the gradient reflected those in the overlying cloud deck (which was sampled with an in-cloud flight leg along precisely the same geographic transect as soon as the below cloud leg was completed). The basic assumption implicit in this procedure is that the mean MBL vertical mixing timescale is short (~1 hr or less) compared to the horizontal mixing transverse to the mean wind (5–10 hr). Usually, a sounding was conducted from the surface to well above the cloud top at each end of the traverses to sample the vertical thermodynamic structure of the MBL along the traverse. After each flight, the cloud albedo along each in cloud flight path was retrieved from satellite data. A synopsis of the flight plan is shown in Fig. 1b.

3. Results and discussion

3.1. *Horizontal gradients*

In the course of the CARMA-II campaign, 13 research flights were conducted by the Twin Otter while, during CARMA-III, 16 flights were undertaken. Of these, six during CARMA-II and six during CARMA-III contained usable data on mesoscale (meso-β scale or ~100 km) gradients. These flights are summarized in Table 1.

The observed gradients, below cloud, in cloud and from remotely retrieved parameters all show substantial interflight variability in their spatial patterns. In some flights the trends in parameters are nearly monotonic along the traverses, in others, quite erratic. Most significantly, in some cases below cloud and in cloud parameters are well correlated with retrieved albedo, supporting a dependence of the albedo on, for example, aerosol concentration or SST, while in other cases little correlation was found. Examples of these various patterns are shown in Figs 2–5. It should be noted that in most of the examples incorporated into the detailed analysis, HYSPLIT-IV back-trajectories indicated N–NW marine air for 96 hr prior to sampling. Exceptions are Flight 708, for which the trajectory briefly passed over land 18 hr prior to sampling, and Flight 818, which had a trajectory from off shore of the Los Angeles Basin (effectively continental air) with a traveltime of ~20 hr. This compares with a vertical mixing timescale (to moisturize the advected air to normal marine conditions) of ~24 hr. (Stull, 1988)

It is important to note that the HYSPLIY-IV trajectories were initialized at several different altitudes to test the sensitivity of the results. Typically, the initial altitudes were 30 m, 200 m and

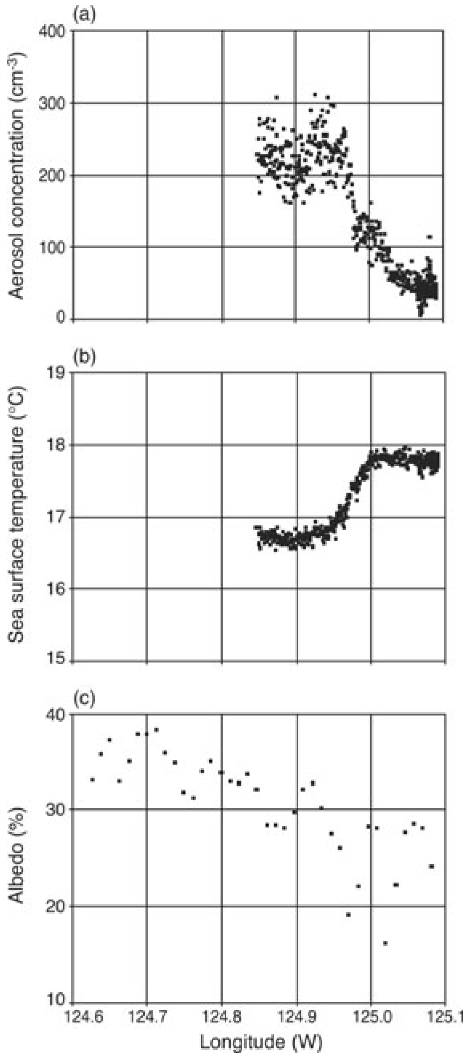

Fig. 2. Horizontal gradients observed on Flight 816 for (a) aerosol concentration, (b) SST and (c) albedo.

whatever the inversion height was for a particular case. No significant differences in trajectory with initial altitude were found.

In Fig. 2, data from Flight 816 show significant coherence (i.e., similar spatial trends) between the albedo and the subcloud aerosol number concentration. On the other hand, the SST trend is relatively small (∼1 °C over ∼20 km) and in the opposite sense to what would be expected to modulate the observed change in albedo (cf. Hegg et al., 2004). The in-cloud trends (not shown but summarized in Table 4), in accord with this, show a high degree of correlation of the CDNC with the subcloud aerosol (linear correlation coefficient, $r = 0.89$, fractional probability of chance correlation, $p = 0.05$) but the liquid water content (LWC) has no clear trend. Hence, this case provides an example of the first type of indirect aerosol forcing (Twomey effect).

In contrast to this, Flight 709 (Fig. 3) shows an albedo correlated with SST ($r = 0.84$, $p = 0.01$) but weakly anti-correlated with the aerosol gradient ($r = –0.31$), and with the CDNC gradient. Flight 712 also displays coherence between albedo and SST gradients ($r = 0.96$, $p = 0.003$) but with no significant aerosol gradient present (albedo-aerosol correlation $r = –0.018$, $p = 0.76$). Despite this, the CDNC as well as the LWC track the SST change, suggesting a larger fraction of the aerosol are activated at the west end of the traverse where CDNC, drizzle and cloud albedo are highest (or, possibly, precipitation scavenging).

Other, more complex, scenarios can also be found. For example, in Flight 708, the below cloud gradients in aerosol and SST are coherent (i.e., change in the same sense), leading to a joint, and very strong, modulation of cloud albedo (Fig. 4). The >60% increase in aerosol concentration coupled with the 2.5 °C SST warming along the traverse yield a nearly factor of 3 enhancement in cloud albedo. Finally, Flight 826 shows an albedo trend in the opposite sense to the aerosol gradient with no clear gradient in SST (Fig. 5). For this interesting case, the 50% reduction in cloud albedo to the west is due largely to a decrease in the cloud geometric height (based on vertical profiles at each end of the traverse) as well as LWC and thus cloud drop effective radius.

This phenomenology has been previously remarked by Brenguier et al. (2003) for the ACE-2 data set. Furthermore, Han et al. (2002), using an extensive satellite data set have shown that cloud liquid water paths (LWPs) in marine stratiform clouds are commonly negatively correlated with columnar CDNC. However, the explanation offered for the ACE-2 observations, concurrent advection of particle-rich but dry continental air, does not appear to explain our observations, either for Flight 826 in particular, or in general.

As previously mentioned, HYSPLIT model back trajectories for the majority of our flights (and all along the traverse for Flight 826) are entirely marine for 96+ hr prior to sampling. Nevertheless, this is a far from conclusive criterion and it is worthwhile to explore this possibility further, particularly since quite small differences in the below cloud moisture content can produce significant differences in cloud LWPs. To access this possible explanation more fully, we have examined the correlation between aerosol number concentration and both total water mixing ratio (r_{tot}) and moist static energy (MSE) along the below cloud traverses. Values for the correlations are given in Table 1. For the ACE-2 scenario to be in effect, one would expect a substantial negative correlation between the particle number and either of the thermodynamic parameters. However, while negative correlations are present in about half of the traverses, with one exception they are quite low, explaining 6% or less of the variance between the correlation variables. The one exception, Flight 816, while showing a very substantial negative correlation, also shows a high coherence between the trend in aerosol number concentration and cloud albedo (to be discussed below), that is, the ACE-2 hypothesis is unnecessary since there is no anomalous relationship between aerosol concentration and albedo that requires an explanation. Overall then, the ACE-2

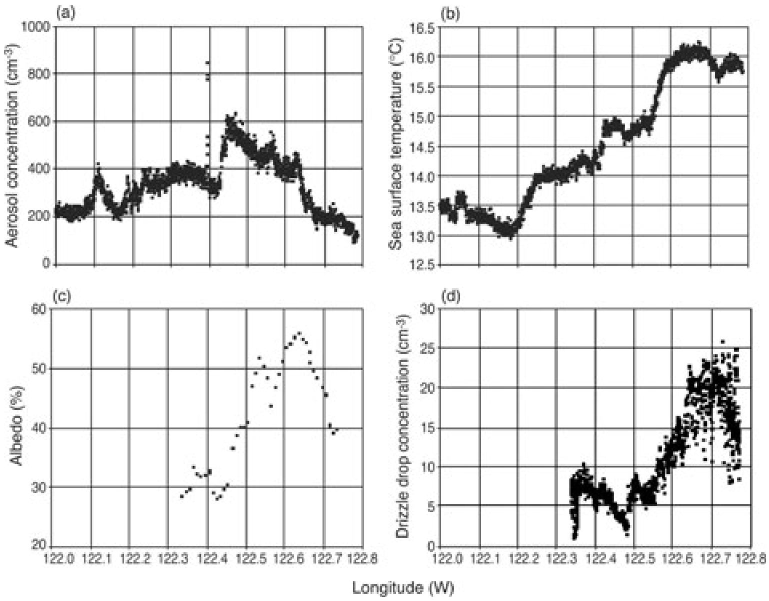

Fig. 3. Horizontal gradients observed on Flight 709 for (a) aerosol concentration, (b) SST, (c) albedo and (d) drizzle drop concentration.

scenario does not seem applicable to either Flight 826 or our data set as a whole, although the sensitivity of the LWP (as well as the LWC and cloud top effective radius) to quite small changes in the subcloud water mixing ratio ($\sim$0.1 g kg^{-1}) make it difficult to categorically reject this hypothesis.

The explanation offered by Han et al. for their observations, a negative modulation of LWP by precipitation via decoupling also does not seem applicable in our case. It is contrary to many (though not all) model predictions and is in any case unlikely in the shallow coastal MBL examined here (cf. Bretherton and Wyant, 1997). Certainly, there is no evidence of decoupling in Flight 826 or, indeed, in any of the cases presented in this study. For example, in Flight 826, the MSE is virtually constant with height below the inversion, having a value of 310 KJ kg^{-1} with a *SD* of 0.3 KJ kg^{-1}. Similarly r_{tot} has a MBL mean of 9.1 g kg^{-1} with a *SD* of 0.2 g kg^{-1}. This situation is characteristic of a well-mixed MBL and is typical of our data. Decoupled MBL's show far more vertical variation in these conserved variables (cf. Martin et al., 1995). It is also conceivable that the east-west contrast is simply due to more favourable thermodynamic conditions at the Eastern end of the traverse, leading to larger H and enhanced precipitation. However, as suggested by the correlations of r_{tot} and MSE with aerosol concentration shown in Table 1, conditions are actually more favourable to the west. The explanation for the trend observed in Flight 826 appears rather to be along the lines recently formulated by Ackerman et al. (2004) who find that the decrease in sedimentation and precipitation due to higher CDNC enhances entrainment through the MBL inversion. Indeed, suppression of sedimentation alone will have this effect according to very recent simulations with an LES model (Bretherton, personal communication, 2006), essentially by enhancing the liquid water available for evaporative cooling in the subinversion mixing zone. If the superinversion air is quite dry, the resultant enhanced instability and mixing of dry air can dry out the cloud layer. From east to west along the traverse the CDNC increases from 200 to 350 cm^{-3} leading to a reduction in drizzle to virtually zero (no drizzle drops present at all) and a decrease in the mean drop size. This leads, as per Ackerman et al., to enhanced entrainment of dry, superinversion air, a consequent drying of the cloud layer, which decreases in geometric thickness by 45% and in LWC by 50% (Fig. 6). The superinversion RH of 36% and the decrease in water vapor mixing ratio across the inversion of 3.7 g kg^{-1} are actually quite close to the example from FIRE-I used by Ackerman et al. to illustrate their proposed mechanism. The resulting decrease in cloud albedo is in accord with the drying.

These examples illustrate that there are a number of factors that modulate the albedo of marine stratocumulus, that their interaction can be complex, and that no single factor, such as aerosol number concentration, is generally predominant. Qualitative analysis of horizontal gradients alone, as indeed suggested by the case of Flight 826, is unlikely to lead to a better understanding of albedo modulation. Hence, we next turn to a more quantitative analysis of the data set and examine the vertical structure of the cloud deck as well.

3.2. Vertical profiles

The cloud decks studied here are quite uniform, having few breaks and little variation in cloud top altitude. For these decks, with optical depths $\geq$5, cloud albedo is essentially a function of cloud optical depth alone (cf. Lacis and Hansen, 1974) and the optical depth can, in turn, be simply expressed as:

$$\tau = 2\pi H \bar{N} r^2, \quad (1)$$

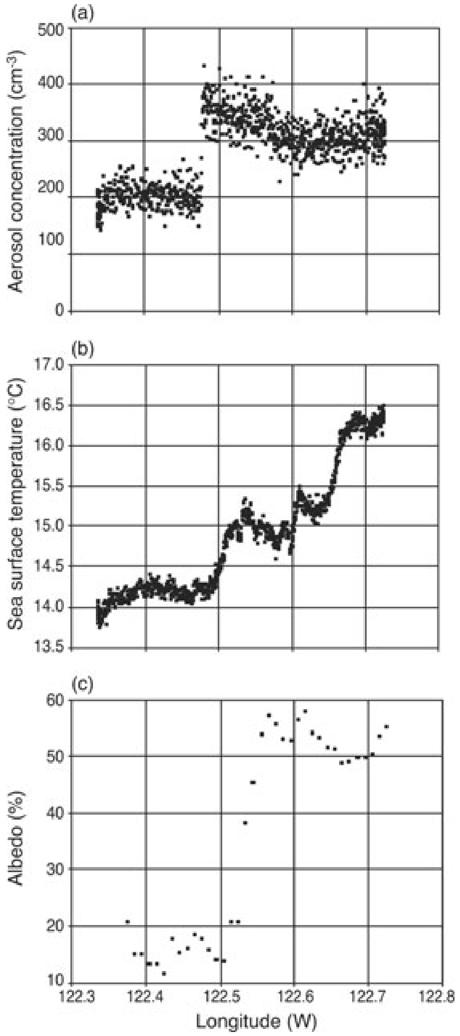

Fig. 4. As in Fig. 2 but for Flight 708.

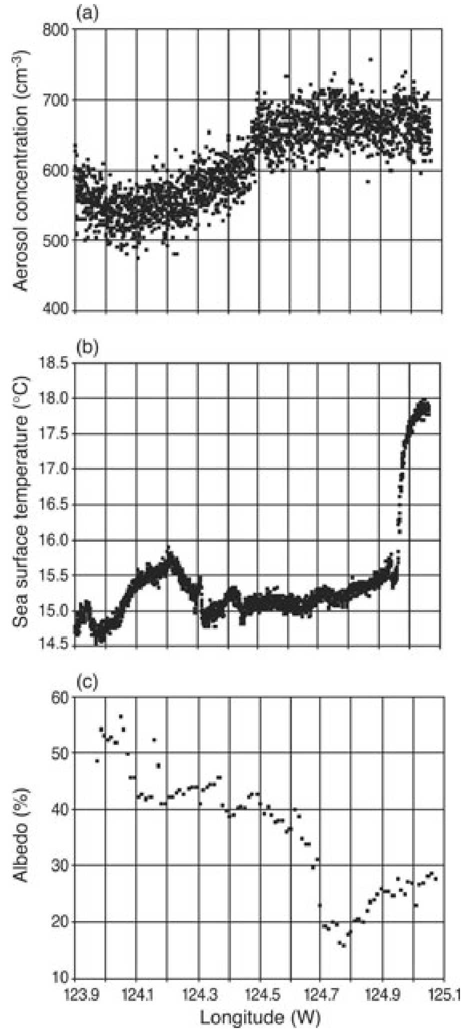

Fig. 5. As in Fig. 2 but for Flight 826.

where H is the cloud geometric thickness (defined here as the interval over which CDNC $\geq$ 2 cm^{-3}), $\bar{N}$ the mean CDNC over that thickness, and r the mean cloud drop radius for that thickness (cf. Hobbs, 1993; Twomey, 1991).Note that we use the cloud drop effective radius as a surrogate for r since this is directly measured and used in other calculations. This formulation clearly shows the potential independent impact of factors other than CDNC (and thus presumptively aerosol concentration) on the cloud albedo. Of course, as originally proposed by Twomey, the indirect aerosol forcing assumes a constant LWC and H, thus imposing a close and obvious relationship between CDNC and $r_{\mathrm{eff.}}$ (that jointly determine LWC). On the other hand, the dependence of H on CDNC is much less clear. Numerous previous studies have in fact sought such a dependence (usually in terms of precipitation modulation) in order to examine the dependence of cloud albedo on CDNC alone (e.g., Pincus and Baker, 1994; Hegg et al., 1996). However, as per our previous discussion, there is evidence that H and CDNC do not always vary together as postulated (i.e., positively correlated). To briefly reiterate, Brenguier et al. (2003) found that, for the ACE-2 operations area, higher CDNC was associated with high aerosol concentrations due to the advection of continental pollution. Since the advected air was also appreciably drier than the background marine air, smaller cloud thickness was associated with the higher CDNC. Similarly, Shao and Liu (2005) found that, for the near shore (within 1000 km) portion of the California stratocumulus deck, the relationship between H and CDNC was inverse, in agreement with the analysis of Brenguier et al. and contrary to what would have been expected from older formulations of indirect forcing by aerosols. Finally, Han et al. (2002) found an inverse correlation between the LWP (a function of CDNC and r_{eff}) and columnar CDNC in about one third of their data set though, as discussed above, the proffered explanation does not seem applicable to our data.

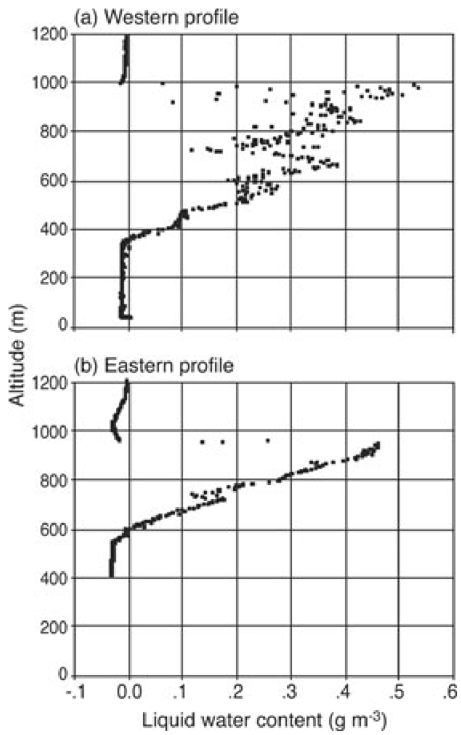

Fig. 6. Liquid water vertical profiles for the (a) east and (b) west ends of the horizontal traverse from Flight 709.

To explore this issue with the current data set, the parameters in eq. (1) have been calculated from the flights listed in Table 1. Sixteen vertical profiles through the regional stratocumulus deck were taken during which all of the requisite instrumentation was properly functioning (e.g., Flights 710, 810 and 819 were not included due to a lack of good albedo retrievals). Mean parameters characterizing the profiles are reported in Table 2. In addition to the parameters necessary to evaluate the optical depth using eq. (1), the below cloud aerosol concentration derived from the PCASP-100× is given, as is the drizzle drop concentration (drops with diameter greater than 100 μm), the retrieved and calculated albedo, and the horizontal mean CDNC for a roughly 10 km portion of the horizontal traverse centred on the vertical profile. This last parameter permits at least an ad hoc assessment of how representative the profiles are of the surrounding cloud and is derived simply to ensure that the profiles are not anomalous. The linear correlation coefficient between the profile and horizontal CDNC is 0.92, supporting the representativeness of the profiles.

Preliminary to examining the relationships between, and impact of, the parameters shown in Table 2 on cloud albedo, it is useful to compare the albedo derived from them via eq. (1) and the albedo retrieved from satellite radiometers. A reasonable degree of closure between the retrieved and calculated albedo's would confirm the utility of eq. (1) as a useful form for the relationship between the parameters that determine the cloud albedo. A regression of retrieved onto calculated albedo using the data in Table 2 yields a regression equation:

$$\text{Aret} = (0.61 \pm 0.13)\text{Acalc} + (5.0 \pm 7.7) \quad (2)$$

with an R^2 value of 0.60 ($p < 0.001$). The residual variance associated with A_{ret} is surprisingly high and there is a significant bias in the slope (gain bias). Nevertheless, most of the variance is explained by the parameters in Table 2 and supports the usage of eq. (1) as a framework for discussing the factors impacting cloud albedo.

Table 2. Parameters derived from the vertical profiles obtained during the CARMA-II and CARMA-III campaigns

Flight	Location	Albedo calc.	Albedo o retrieved	CDNC (cm^{-3})	r_{eff} (μm)	H (m)	Optical depth	Drizzle drops[a] (cm^{-3})	CDNC horizontal mean	Below Cloud Aerosol (cm^{-3})
708	East	44	20	50	6.3	490	6.1	10	50	200
708	West	81	55	275	6.8	410	33.0	7	250	325
709	East	59	47	300	4.4	300	10.9	7	400	380
709	West	72	44	125	6.3	630	19.6	20	180	180
712	East	76	43	250	5.8	450	23.8	3	250	375
712	West	73	50	400	5.8	240	20.3	1.5	400	380
713	East	25	19	350	3.8	80	2.5	1	400	380
713	West	43	44	350	4.2	150	5.8	1	400	380
721	East	52	36	250	4.2	300	8.3	4.5	325	300
721	West	47	38	325	4.2	190	6.8	2.5	300	300
816	East	67	40	250	5.1	380	15.5	9	150	250
816	West	47	30	130	5.8	250	6.9	20	80	70
818	West	42	22	40	7.4	400	5.5	30	30	50
824	West	61	53	300	4.7	290	12.1	8	300	1000
826	East	58	53	200	5.3	300	10.6	12	225	550
826	West	45	28	350	4.2	165	6.4	1.5	350	650

[a]Cloud drops with diameter >100 μm.

Examination of the covariance of the parameters in Table 2 reveals several points relevant to the issue at hand. First, of course, there are a number of expected relationships. The CDNC has a very significant negative correlation with the drizzle drop concentration (–0.85, $p = 0.01$), CDNC is also negatively correlated with the effective radius (–0.7, $p = 0.01$) but positively correlated with the subcloud aerosol concentration (0.55, $p = 0.05$). On the other hand, contrary to conventional expectation, the cloud geometric thickness has a very significant negative correlation with the CDNC (–0.68, $p = 0.01$). This correlation is similar to that found by Brenguier et al. (2003) for the ACE-2 data set but, as discussed above, it is unlikely to be attributable to the influence of relatively dry, continental air. As might be expected from this, there is also a negative, but weaker, correlation between the below cloud aerosol concentration and the cloud thickness (–0.34, $p = 0.2$). The large-scale satellite data set of Shao and Liu (2005), which encompasses the CARMA locale, also suggests this sort of relationship. However, direct comparison is difficult because Shao and Liu had to use the aerosol optical depth as a proxy for the below cloud aerosol concentration, and, furthermore, could not use simultaneous measurements of even this parameter with the cloud properties since, of course, the presence of cloud precluded aerosol optical depth retrieval. Indeed, the utilization of climatological mean aerosol optical depths constitutes, in our view, a major uncertainty in the findings of this study. In light of the significance of its findings, we feel it worthwhile to test some of the Shao and Liu results using our in situ data.

A prominent finding of Shao and Liu, and one that affords an opportunity for comparison with previous work, is the relationship between the aerosol optical depth, the cloud geometric thickness and the cloud drop effective radius. Shao and Liu test the relationship proposed earlier by Nakajima et al. (2001), namely,

$$r_{\text{eff}} = \sigma \tau_a^{-\alpha} H^{\beta}, \tag{3}$$

using multiple linear regression of the logarithm of eq. (3). We do the same but now using the in situ concentration of aerosol in place of the climatological aerosol optical depths. The results of this analysis are reported in Table 3, together with the Shao–Liu findings. When using both the aerosol optical depth (or the aerosol number concentration in our case) and the cloud geometric thickness as regression variables, the values for α and β are statistically indistinguishable for the two studies. When the aerosol optical depth (or number concentration) alone is used as an independent variable, our α value (0.16 ± 0.06) is significantly lower than that of Shao and Liu but virtually identical to that reported earlier by Nakajima et al. (2001), 0.17, a value with which Shao and Liu feel their result is comparable. Hence, overall, our analysis based on in situ measurements compares quite favourably with the previous satellite work reported and confirms the utility of the more indirect approach. It also, once again, suggests the importance of the cloud geometric thickness in determining the cloud albedo and is consistent with the lack of positive correlation between the cloud thickness and the aerosol optical depth. This leads us back to the question of the influence of aerosol concentration on H as proposed by Ackerman et al., in contrast to the positive correlation expected from more conventional conceptions that constrain H to increase with CDNC or be independent of it.

From the 16 profiles shown in Table 2, six matched pairs of profiles, each from the same traverse but at essentially opposite ends, with substantially different parameter values, can be extracted. Note that, in principle, a seventh pair could be taken from Flight 713. However, this case displays no aerosol gradient, no gradient in either CDNC or drizzle, and the drizzle concentration is very low. It is clearly a case where the SST gradient is the highly dominant factor in modulation of the albedo and we therefore do not include it in this analysis. The six matched pairs, together with various parameter values necessary to test the applicability of the Ackerman et al. mechanism to the CARMA data set are given in Table 4. In all cases the relationship between the precipitation and the CDNC is as expected, negative covariance. However, in only one of the cases (816) is the relationship between the CDNC and the cloud thickness as expected from conventional theory, though in one other (708) the cloud thickness changes only modestly (~16%). In the four remaining cases, the cloud thickness decreases with increasing CDNC and decreasing precipitation. Of course, in some cases (e.g., Flight 709), this is likely due in part to influence of the SST gradient on cloud LWP. However, the phenomenology is also more in accord with the Ackerman et al. scenario. In this regard it should be noted that these four cases have appreciably lower super-inversion RH's (22–39% compared to 52–57%) and much larger decreases in the water vapor mixing ratio across the

Table 3. Regression parameters for the analysis of the relationship between cloud drop effective radius and cloud thickness, and a measure of aerosol concentration. Symbols as defined in eq. (3)

Regression variables	Study	R^2	α	β	Constant [ln(σ)]
ln τ_a, ln H	Shaoand Liu	0.73	–0.07 ±0.03	0.24 ± 0.02	2.48
ln τ_a	Shao and Liu	0.44	–0.30 ±0.03	–	1.70
ln N_a, ln H	This study	0.71	–0.10 ±0.04	0.25 ±0.06	0.80 ±0.5
ln N_a	This study	0.34	–0.16 ± 0.06	–	2.54 ± 0.34

Table 4. Parameter values derived from vertical profiles at the ends of traverses that show the relationship between the cloud properties and the super-inversion properties. (Note that the primary variables, CDNC, H and Drizzle have measurement uncertainties of ±15% or less, ±6% or less and ±80% or less)

Flight	Profile	CDNC (cm^{-3})	H (m)	$\Delta H/H$[a] (per pair)	Drizzle (cm^{-3})	ΔAlbedo (for pair)	Super-inversion RH (%)	Δw_{inv}[b] ($g\ kg^{-1}$)
708	W	275	410	–0.16	7	.35	57	3
	E	50	490		10			
709	W	125	630	–0.52	20	.03	31	8
	E	300	300		7			
712	W	400	240	–0.47	1.5	.07	22	10.8
	E	250	450		3.0			
721	W	325	190	–0.37	2.5	.02	37	9.7
	E	250	300		4.5			
816	W	130	250	0.52	20	.10	52	2.5
	E	260	380		9			
826	W	350	165	–0.45	1.5	–.25	39	7.1
	E	200	300		12			

[a]Fractional change in H relative to the change in CDNC, that is, a negative change means a change in the opposite sense from the change in CDNC.
[b]The values are mean values along each traverse. It should be noted that there was very little variation over the traverses.

inversion (~9 g kg^{-1} compared to ~3 g kg^{-1}) than do the two cases which display a more conventional phenomenology. For example, Flight 709 has a superinversion RH of 31% and a decrease in mixing ratio of 8 g kg^{-1} across the inversion. This leads to a change in the LWC profile qualitatively similar to that predicted by the Ackerman et al. model for similar conditions. These observed profile changes are shown in Fig. 6. While firm conclusions cannot be drawn from the limited number of cases presented here, these results do suggest that the Ackerman et al. scenario is not rare and could contribute appreciably towards contravention of conventional aerosol-cloud relationships.

The significance of the potential disjoint between the increasing CDNC and the decreasing cloud thickness is that the opposing tendencies will attenuate the impact of aerosols on the cloud optical depth and thus the albedo. Quantification of this effect, however, is difficult; first simply because its occurrence will depend on the mesoscale thermodynamic structure of the system, for example, the super inversion humidity; second, because it will depend on the magnitude of the aerosol concentration as compared to these other thermodynamic parameters (cf. Ackerman et al.). Nevertheless, with a few ad hoc assumptions we make a first attempt at such quantification. Based on eq. (1) and the data in Table 2, we first calculated the fractional change in the albedo per fractional change in the CDNC [($\Delta \ln A/\Delta \ln$ (CDNC))]. We then calculate the same parameter but now artificially holding the cloud thickness constant for the five cases in which it actually decreases, that is, we assume that the increase in the CDNC does not affect cloud thickness. (It is important to note that this procedure is not a formal partial derivative but rather a physical assumption.) Obviously such is not the case for either the Ackerman et al. or conventional scenario, and does not give the entire difference to be expected from the contrasting mechanisms since the convention approach will probably lead to increased cloud thicknesses. Nevertheless, it will likely give a lower bound for the impact of entrainment on albedo and thus provide useful information. The fractional changes with and without the assumption of constant thickness are shown in Table 5. The decrease in cloud thickness engendered by entrainment of dry air as proposed by Ackerman et al. has a very significant impact on the albedo in some of these cases, even reversing the albedo gradient from that expected from the conventional scenario. However, a cautionary note is in order here. Recent work by Stevens et al. (2003) has shown that cloud top entrainment in marine stratocumulus does not always lead to a thinning of the cloud layer if other processes are sufficiently strong to dominate it (e.g., increasing surface moisture flux). As stated earlier, a number of different processes are generally at work in marine stratocumulus and prediction of their net effect is difficult. What the results in Table 5 suggest is simply that aerosols themselves can tend to decrease as well as increase cloud albedo.

Table 5. Calculations of the fractional change in albedo per change in CDNC based on the data in Table 2. The last column is for such a calculation assuming that cloud thickness did not change

Flight	$\Delta \ln A/\Delta \ln$(CDNC)	$\Delta \ln A/\Delta \ln$(CDNC) constant H
708	0.18	0.20
709	–0.13	0.12
712	–0.07	0.15
721	–0.33	0.40
816	0.19	–
826	–0.29	0.04

4. Conclusions

Examination of the horizontal gradients of cloud and subcloud properties on the mesoscale, together with simultaneously retrieved cloud albedo, has demonstrated that, while aerosol concentration certainly can modulate the cloud albedo on this scale, such properties as SST can have a similar impact and the convolution of the impacts of such factors can lead to either attenuation or enhancement of the aerosol effect alone. Additionally, analysis of vertical profiles of cloud properties suggests that aerosol impact on cloud albedo through modulation of cloud drop sedimentation can be either positive or negative as explained by the mechanism recently proposed by Ackerman et al. (2004) and recent LES modeling. As a consequence of this, the impact of aerosols via the second indirect effect (precipitation modulation) can be highly variable and, indeed, may be opposite to that previously proposed, that is, higher aerosol concentrations can lead to thinner clouds with reduced albedo.

The implications of the complexity suggested by the above analysis are potentially quite significant. The models used to quantify and predict the global radiative forcing due to aerosols must necessarily utilize many parameterizations, and apply them on a fairly coarse grid, rarely resolving below the meso-β scale examined in this study. As pointed out by Han et al. (2002), this could have important consequences. Conventional parameterizations, which predict qualitatively similar impact for aerosol for both the first and second indirect effects, namely, increasing aerosol concentration leads to increases in the cloud albedo, likely will over predict the increase in cloud albedo associated with a given change in aerosol concentration when applied at this scale, perhaps substantially and certainly with a magnitude dependent on meteorological parameters that are also poorly characterized on this scale. This, in turn, suggests that current estimates of indirect aerosol forcing could be substantially in error, and that the issues addressed here should be investigated more fully.

5. Acknowledgments

Support for this study was provided by ONR grant N00014-97-1-0132. We wish to thank the staff of CIRPAS for their support, particularly the pilot and co-pilot of the Twin Otter, Mike Hubbell and Roy Woods. We also wish to thank Professors M. Baker and C. Bretherton for useful discussions, and an anonymous reviewer and especially Professor J.-L. Brenguier for useful comments.

References

Ackerman, A. S., Kirkpatrick, M. P., Stevens, D. E. and Toon O. B. 2004. The impact of humidity above stratiform clouds on indirect aerosol climate forcing. *Nature* **432**, 1014–1017.

Albrecht, B. 1989. Aerosols, cloud microphysics, and fractional cloudiness. *Science* **245**, 1227–1230.

Brenguier, J.-L., Pawlowska, H. and Schuller, L. 2003. Cloud microphysical and radiative properties for parameterization and satellite monitoring of the indirect effect of aerosol on climate. *J. Geophys. Res.* **108**, CMP 6-1 to 6-14.

Brenguier, J.-L., Pawlowska, H., Schuller, L., Preusker, R., Fischer, J. and co-authors. 2000. Radiative properties of boundary layer clouds: Droplet effective radius versus number concentration. *J. Atmos. Sci.* **57**, 803–821.

Bretherton, C. S. and Wyant, M. C. 1997. Moisture transport, lower-tropospheric stability, and decoupling of cloud-topped boundary layers. *J. Atmos. Sci.* **54**, 148–167.

Charlson, R. J., Lovelock, J. E., Andreae, M. O. and Warren, S. G. 1987. Oceanic phytoplanckton, atmospheric sulphur, cloud albedo and climate. *Nature* **326**, 655–661.

Durkee, P. A. and co-authors 2000. The impact of ship-produced aerosols on the microstructure and albedo of warm marine stratocumulus clouds: A test of the MAST hypotheses 1i and 1ii. *J. Atmos. Sci.* **57**, 2554–2569.

Ferek, R. J., Garrett, T., Hobbs, P. V., Strader, S., Johnson, D. and co-authors. 2000. Drizzle suppression in ship tracks. *J. Atmos. Sci.* **57**, 2707–2728.

Han, Q., Rossow, W. B. and Lacis, A. A. 1994. Near-global survey of effective droplet radii in liquid water clouds using ISCCP data. *J. Clim.* **7**, 465–497.

Han, Q., Rossow, W. B., Zeng, J. and Welch, R. 2002. Three different behaviors of liquid water path of water clouds in aerosol-cloud interactions. *J. Atmos. Sci.***59**, 726–733.

Hegg, D. A., Durkee, P. A., Jonsson, H. H., Nielsen, K. and Covert, D. S. 2004. Effects of aerosol and SST gradients on marine stratocumulus albedo. *Geophys. Res. Lett.* **31**, L06113.

Hegg, D. A., Gao, S. and Jonsson, H. 2002. Measurements of selected dicarboxylic acids in marine cloud water. *Atmos. Res.* **62**, 1–10.

Hegg. D. A., Hobbs, P. V., Gasso, S., Nance, J. D. and Rangno, A. L. 1996. Aerosol measurements in the Arctic relevant to direct and indirect aerosol radiative forcing. *J. Geophys. Res.* **101**, 23349–23363.

Hobbs, P. V. 1993. Aerosol-Cloud Interactions. In: *Aerosol-Cloud-Climate Interactions*. (Eds. P. V. Hobbs). Academic Press, New York, p. 233.

Hudson, J. G. and Frisbie, P. R. 1991. Cloud condensation nuclei near marine stratus. *J. Geophys. Res.* **96**, 20 795–20 808.

Klein, S. A. Hartmann, D. L. and Norris, J. R. 1995. On the relationships among low cloud structure, sea surface temperature, and atmospheric circulation in the summertime northeast Pacific. *J. Clim.* **8**, 1140–1155.

Lacis, A. A. and Hansen, J. E. 1974. A parameterization for the absorption of solar radiation in the earth's atmosphere. *J. Atmos. Sci.* **31**, 118–133.

Martin, G. M., Johnson, D. W., Rogers, D. P., Jonas, P. R., Minnis, P. and co-authors. 1995. Observations of the interaction between cumulus clouds and warm stratocumulus clouds in the marine boundary layer during ASTEX. *J. Atmos. Sci.* **52**, 2902–2922.

Martin, G. M., Johnson, D. W. and Spice, A. 1994. The measurement and parameterization of effective radius in warm stratocumulus clouds. *J. Atmos. Sci.* **51**, 1823–1842.

Nakajima, T., Higurashi, A., Kawamoto, K. and Penner, J. E. 2001. A possible correlation between satellite-derived cloud and aerosol microphysical parameters. *Geophys. Res. Lett.* **28**, 1171–1174.

Pincus, R. and Baker, M. B. 1994. Effect of precipitation on the albedo susceptibility of clouds in the marine boundary layer. *Nature* **372**, 250–252.

Pincus, R., Baker, M. B. and Bretherton, C. S. 1997. What controls stratocumulus radiative properties? Lagrangian observations of cloud evolution. *J. Atmos. Sci.* **54**, 2215–2236.

Platnick, S. and Twomey, S. 1994. Determining the susceptibility of cloud albedo to changes in droplet concentration with the advanced very high-resolution radiometer. *J. Appl. Meterol.* **33**, 334–347.

Rao, C. R. N., Sullivan, C. J. and Zhang, N. 1999. Post-launch calibration of meteorological satellite sensors. *Adv. Space Res.* **23**, 1357–1365.

Rossow, W. B. C. Delo and Cairns, B. 2002. Implications of the observed mesoscale variations of clouds for the earth's radiation budget. *J. Clim.* **15**, 557–585.

Sekiguichi, M., Nakajima, T., Suzuki, K., Kawamoto, K., Higurashi, A. and co-authors. 2003. A study of the direct and indirect effects of aerosols using global satellite data sets of aerosol and cloud parameters. *J. Geophys. Res.* **108**, AAC4-1 to 15.

Shao, H. and Liu, G. 2005. Why is the satellite observed aerosol's indirect effect so variable? *Geophys. Res. Lett.* **32**, L15802, 1–4.

Stevens, B. et al. 2003. On entrainment rates in nocturnal marine stratocumulus. *O.J.R. Meteorol. Soc.* **129**, 3469–3493.

Stull, R. B. 1988. *An Introduction to Boundary Layer Meteorology*. Kluwer Academic Publishers, Boston, pp.666.

Twomey, S. 1974. Pollution and the planetary albedo. *Atmos. Environ.* **8**, 1251–1256.

Twomey, S. 1991. Aerosols, clouds and radiation. *Atmos. Environ.* **25A**, 2435–2442.

Wang, J., Flagan, R. C., Seinfeld, J. H., Jonsson, H. H., Collins, D. R. and co-authors. 2002. Clear-column radiative closure during ACE-Asia: Comparison of multiwavelength extinction derived from particle size and composition with results from Sun photometry. *J. Geophys. Res.* **107**, AAC7 1–22.

Warren, S. G., Hahn, C. J., London, J., Chervin, R. M. and Jenne, R. L. 1988. Global distribution of total cloud cover and cloud type amounts over the ocean. NCAR/TN-317+STR, NCAR Technical Notes.

Wyant, M. C., Bretherton, C. S., Rand, H. A. and Stevens, D. E. 1997. Numerical simulations and a conceptual model of the stratocumulus to trade cumulus transition. *J. Atmos. Sci.***54**, 168–192.